Accepted Manuscript

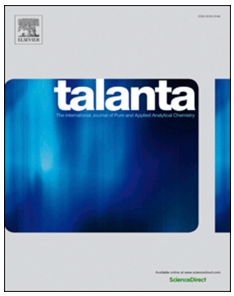

Electrochemical paper-based microfluidic device for high throughput multiplexed analysis

Elson Luiz Fava, Tiago Almeida Silva, Thiago Martimiano do Prado, Fernando Cruz de Moraes, Ronaldo Censi Faria, Orlando Fatibello-Filho

PII: S0039-9140(19)30575-2

DOI: https://doi.org/10.1016/j.talanta.2019.05.081

Reference: TAL 19966

To appear in: *Talanta*

Received Date: 7 May 2019

Revised Date: 17 May 2019

Accepted Date: 18 May 2019

Please cite this article as: E.L. Fava, T.A. Silva, T. Martimiano do Prado, F. Cruz de Moraes, R.C. Faria, O. Fatibello-Filho, Electrochemical paper-based microfluidic device for high throughput multiplexed analysis, *Talanta* (2019), doi: https://doi.org/10.1016/j.talanta.2019.05.081.

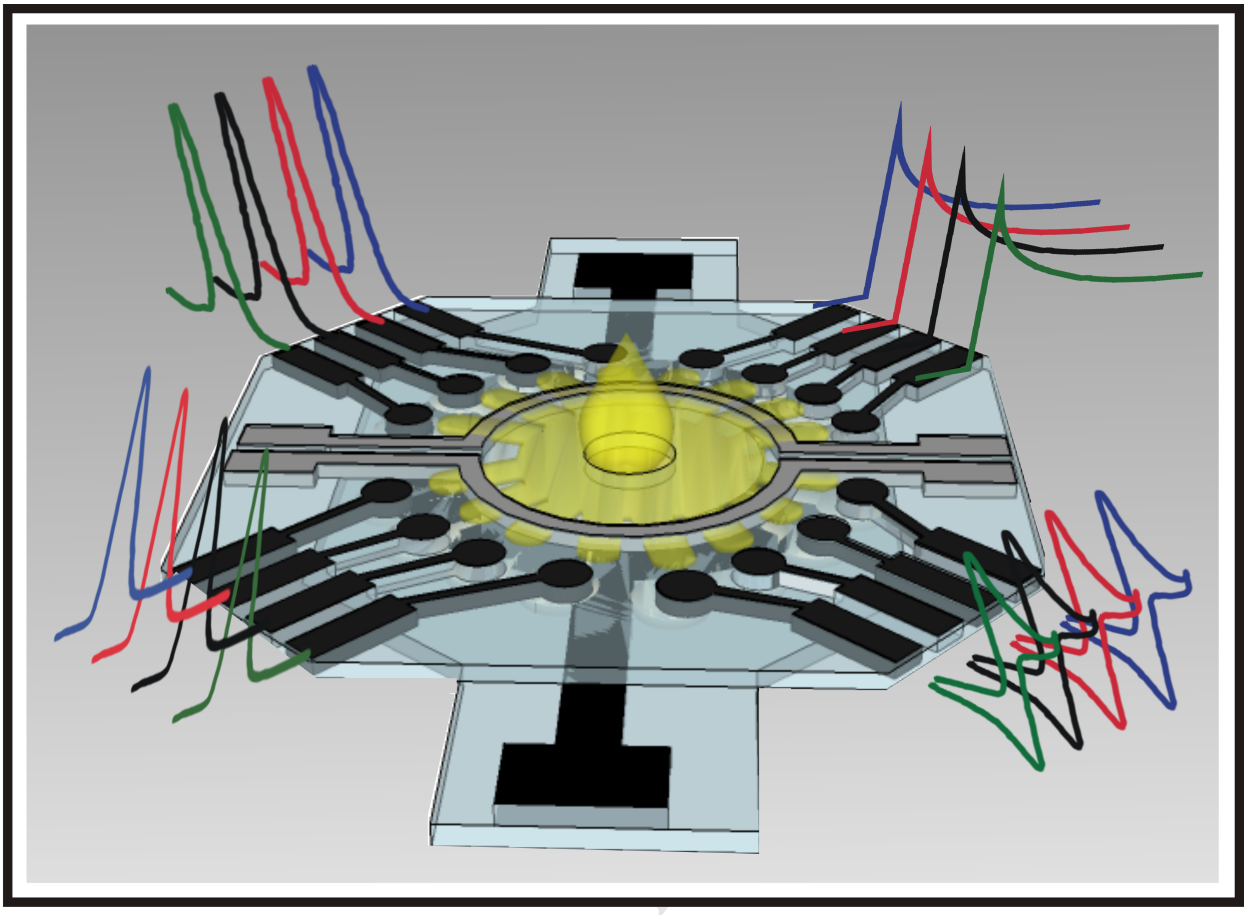

Electrochemical paper-based microfluidic device for high throughput multiplexed analysis

Elson Luiz Fava[a], Tiago Almeida Silva[a, b], Thiago Martimiano do Prado[a], Fernando Cruz de Moraes[a], Ronaldo Censi Faria[a]*, Orlando Fatibello-Filho[a,]*

[a]Department of Chemistry, Federal University of São Carlos, São Carlos, P.O. Box 676, 13560-970, SP, Brazil.

[b]Department of Metallurgy and Chemistry, Federal Center for Technological Education of Minas Gerais, Timóteo, 35180-008, MG, Brazil.

* Corresponding author.

Tel.: +55 16 33518098; Fax: +55 16 33518350

E-mail address: bello@ufscar.br (O. Fatibello-Filho)

E-mail address: rcfaria@ufscar.br (R. Censi Faria)

Graphical Abstract

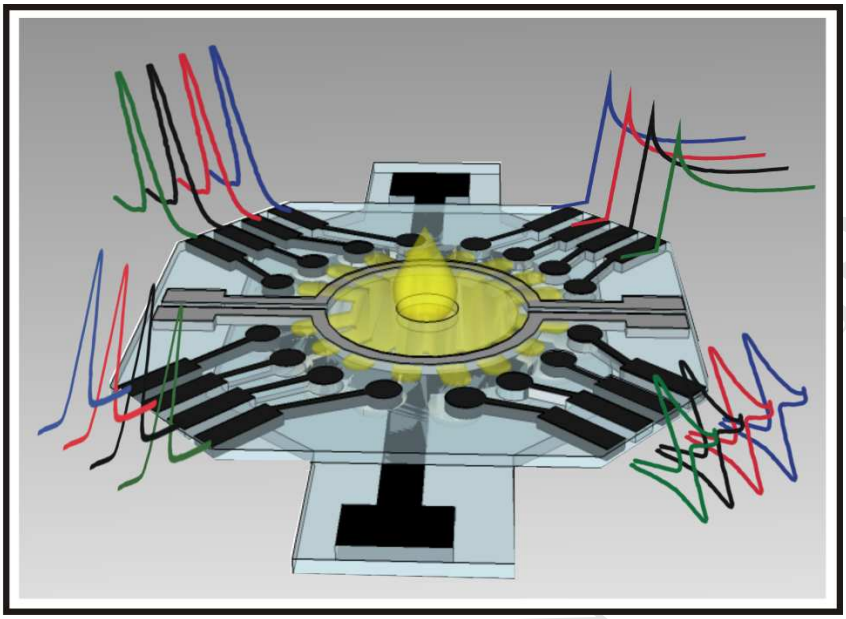

ABSTRACT

A disposable microfluidic electrochemical paper-based device for multiplexed analysis based on sixteen independent microfluidic channels with electrochemical detection is proposed. A major advantage of this work was the non-necessary use of a wax printer for devices manufacturing which has a high cost of operation. In addition, a commercial multiplexing module was used that has the multiplexing capability of 8 to 16 channels and, for the first time using this module, the strategy of multiplexing both the working and reference electrodes were used. These sixteen channels with the respective sensors can be operate employing one or multiple electrochemical techniques with good repeatability and reproducibility for high throughput analysis. As a proof of concept, the electrochemical performance of device was tested with ferrocenecarboxylic acid solution employing cyclic voltammetry, square-wave voltammetry, differential-pulse voltammetry and chronoamperometry. This innovative sensing platform presented capacity of production in large scale and application for clinical tests with safety and short time of assays. A biosensor was constructed using glucose oxidase on the platform for the glucose determination in urine as a non-invasive strategy. The analytical curve was linear in the glucose concentration range from 10^{-4} mol L^{-1} to 4×10^{-2} mol L^{-1}, with limit of detection of 3×10^{-5} mol L^{-1}.

Keywords: Microfluidic; Multiplex analysis; Electrochemical paper-based analysis; Glucose; Urine.

1. Introduction

The development of portable devices for the diagnostics of diseases is being gradually introduced through fast and cheap proposes. In these sense, researchers are doing efforts for the construction of devices that meet the need to perform the analysis in the point of care (POC) [1]. Thus, the analysis occurs where the patient is and with devices as reliable as larger equipment used in the reference methods performed in the central laboratories.

Microfluidic analysis is a promising area for the use of miniaturized devices for diseases diagnosis. In the last years, several works containing microfluidic approach for diseases diagnosis were published [2-6]. Among so many papers, we highlight those aimed the identification of diseases such as HIV, tuberculosis, cancer and Alzheimer's [7-14]. These contributions are very important for the advances in the treatment of these diseases, facing the greater possibility of cure when the early diagnosis is made.

The development of paper based analytical (μPAD) devices involving strategies to create hydrophilic channels in paper in a way to allow the solutions flows by capillarity. The use of wax to create hydrophobic barriers have been largely applied since few steps are required to constructed disposable devices to determination of: total proteins, cholesterol and glucose in biological fluids [15] and heavy metal ions in aqueous solutions [16]. The μPAD devices constructed by wax printing for serological immunoassays were applied for many areas, including food safety, environmental monitoring and veterinary diagnosis [17]. For this, after designed the microfluidic pattern using any drawing software it was printed on the paper using an office wax printer following by a heating step to the wax penetrate in the paper creating hydrophobic barriers. Although their simplicity, the wax printer largely applied to construct μPAD was discontinued by the manufacturer and, currently, there are no other

wax printer available in the market. Based on that new strategy to create microfluidic channels on paper are emerging. Our group developed two methods based on used of cheap craft cutter printer to create microfluidic channels on filter paper. In the first one, the paper was cut in the desired microfluidic pattern and sandwiched on polyester sheets allowing to create 2D and 3D μPADs [18] [19]. The second strategies involve the creation of stamps cutting filter paper in with the microfluidic pattern that was impregnated with wax and used for created hydrophobic barriers by stamping paper following by the thermal treatment for the wax penetrated in the paper. In both cases, disposable μPADs were constructed using simple and low-cost equipment and materials and was successfully applied in chemical analysis.

Usually, the disposable devices for microfluidic analysis are based on methods, which the responses are obtained by colorimetry, fluorimetry or electrochemistry. The first one provides qualitative and/or quantitative information when using image processing software [20-22] while the second method combines several steps of the analytical process with low reagent consumption, reduced analysis time and easy operation [23-25]. The third one provides quantitative information, presents high sensibility, low limit of detection and, in many cases its possible perform simultaneous determination of different analytes [3, 26, 27]. Furthermore, the electrochemical paper-based analytical devices (ePAD) present the possibility of simultaneous determination of two or more analytes in different channels or spots (multiplex analysis); inexpensive and accurate construction steps provided by home cutter printer; and the use of low-cost and disposable materials (e.g. soft cellulose-based filter paper and polyester sheets).

One example is the work proposed by Cincotto *et al.*, in which it was developed a device with two spots for the quantification of different biomarkers. In the spot 1, was deposited graphene quantum dots (GQDs) for the direct oxidation of uric acid, while in

spot 2 GQDs was combined with creatininase enzyme and a redox mediator for the creatinine oxidation [28]. In a low-cost strategy, Oliveira and collaborators created a wax barrier and screening-printing electrodes on paper for multiplexed detection of different drugs [29]. Other interesting strategy employed electrochemical sensor 3D paper-based origami for different types of pesticides [30]. This kind of device also was too used in the immunoassay for the C-reactive protein on screen-printed carbon modified electrode [31]. Moreover, there are several strategies for the application of paper-based devices for biomarkers sensing through aptamers [32], optodes [33] and label-free impedimetric immunosensors [34].

In this scenario, the main objective of this work is the development of a microfluidic device with electrochemical response for unique aliquot of a physiological sample with multiple replicates at same time, and with high sensitivity and good repeatability. The proposed microfluidic paper-based device for multiplexed analysis (Multi-µEPaD) was applied for the detection of glucose in urine sample. This innovative propose allows the analysis with robust and safe results acquired through multiple replicates (16-channels) in a single run. Additionally, the use of an unique aliquot avoids the excessive dispose of contaminated collectors and samples.

2. Experimental section

2.1. Materials, reagents and instrumentation

For the Multi-µEPaD fabrication, it was used polyester sheet (Folien, USA), vinyl adhesive (Imprimax, Brazil), carbon and silver/silver chloride inks (Gwent Group, UK) and a CAMEO 3 Silhouette clipping printer (Silhouette, USA) managed by the Silhouette Studio V3 software. The working electrodes (WEs) were subjected to a

modification step using carbon black (CB) nanoparticles type VXC-72R, kindly supplied (Cabot Corporation, USA), chitosan (CTS) biopolymer, glucose oxidase enzyme (GOx from *Aspergilus Niger*, 155 KU per gram), ferrocenecarboxylic acid (FCA) and D-(+)-glucose were purchased from Sigma-Aldrich.

Electrochemical measurements were carried out with an Autolab PGSTAT12 model potentiostat / galvanostat equipped with the multiplexing module (MUx) (16 channels) and driven by the NOVA® 2.2 software. Multiplexed analysis was performed through Cyclic voltammetry (CV) (*scan rate* = 50 mV s^{-1}); Square wave voltammetry (SWV) (*frequency* = 80 Hz; *amplitude* = 90 mV and *potential increment* = 1 mV); Differential pulse voltammetry (DPV) (*scan rate* = 5 mV s^{-1}, *amplitude* = 90 mV and *modulation time* = 5 ms) and chronoamperometry (*applied potential* = 200 mV).

2.2. Multi-µEPaD *construction*

2.2.1. Microfluidic channel

One of the most important part of the designed device is the respective microfluidic pattern, once through it the samples are transported to the electrochemical cell for analysis. The use of a simple craft cutter printer to cut the filter paper in the desired microfluidic channel instead of use a currently discontinued wax printer is a great advantage to produce µPAD. The #1 Whatman filter paper was used and cut by using the CAMEO 3 Silhouette clipping printer. In this research, different microfluidic patterns were studied. Considering this information the arrangement of the electrodes for multiplexed analysis depends on the adjustment of the microfluidic channels design and its functionality. Two microfluidic patterns were projected. Initially, it was intended to build four sequential electrochemical cells per microfluidic channel with a total of four channels totalizing sixteen sensing points as shown in Fig. S1 (a) (Supporting

material). The insight for this device design was initially in a non-microfluidic ePaD with paper assembled on the crossing points on the electrode column forming a sensor array [35] However, this model soon proved inappropriate. In this study, a 1.0×10^{-3} mol L^{-1} Allura red dye solution was added in the sample spot and the color of gradually decreased along the microfluidic channel, as is shown in Fig. S1, leads to an unwanted non-homogeneous solute distribution between the channels, affecting thus the analytical signal, repeatability and/or reproducibility.

Then, a 16-channels circularly distributed around to the sample spot was designed. The circular distribution of the channels around to the sample injection point provides a radial elution, with homogeneous distribution of the solute into the 16 equidistant detection spots where the sample is analyzed. The proposed microfluidic pattern (hexadecagon mode is shown in the Fig. 1 (a). The flow's homogeneous behavior from the sample injection point to sensing points was demonstrated using a 1.0×10^{-3} mol L^{-1} Allura red dye solution (Fig. 1 (b)). It is worth noting also that a solution volume of only 65 μL was injected and the filling time of the entire microfluidic device occurred at less than 2.5 minutes (Fig. (b)).

Insert Fig. 1

2.2.2. Electrodes

The electrodes using on Multi-μEPaD were constructed based in a simple screen-printed method previously reported [36] [37]. In Fig. 2 are schematically shown the steps of construction of the electrodes. The electrodes were constructed using a vinyl adhesive mask containing the desired pattern of each electrode that composed the electrochemical cell; as working electrodes (WEs); counter electrodes (CEs) and pseudo-reference electrodes (REs). The format of each electrode on the adhesive mask

was achieved from a printing cut process carried out with the cutter printer. The obtained masks were attached to a polyester substrate (in this case, transparency film for laser printers) and directed to the process of applying the carbon conductive ink. Thus, it was deposited on the designed vinyl adhesive mask the carbon conductive ink followed by heat treatment at a temperature of 90°C for 30 minutes. Specifically, in the case of REs, an additional step consisting of deposition of silver / silver chloride conductive ink layer on the previous carbon ink layer followed by a curing process (heating at 60°C for 30 min) was performed.

Insert Fig. 2

The WEs and REs designs are shown in Fig. 3 (a). These components were created to be adapted to the hexadecagon microfluidic pattern. Thus, they were made in the same layer to guarantee the equal distance between WEs and REs, without the need for alignment during assembly of the device. Each of the sixteen WEs have independent electrical contacts so that they can be adapted to the multiplexed analysis module. The electrodes arrange in the Multi-µEPaD allowed that the individual measurements of each WE can be made using different electrochemical techniques in the same device. Each set of four WEs have one RE, totalizing four REs in the device. The electrochemical assays were possible using a commercial multiplex module (MUX-SCNR8) with 8 channels for Autolab PGSTAT. With the MUX module, it is possible to multiplex the PGSTAT electrode connections, where measurements on several electrochemical cells or working electrodes can be done sequentially. In this work, two MUX-SCNR8 coupled (Fig. S2 (a)) were used and at first time the WEs and REs was multiplexed for our device containing 16 electrochemical cells.

The scheme of CE is shown in Fig. 3 (b). It was designed to fit in the previously sheet containing the WEs, REs as well as the microfluidic pattern. The electrode was engineering in a way to keep in contact with all sixteen individual electrochemical cells and maintaining an equal distance between WE and RE of each cell. Thus, analytical signals can be obtained with good repeatability.

Insert Fig. 3

2.2.3. Multi-µEPaD *assembly*

The device was assembled by overlapping of each component's layer. The sealing of Multi-µEPaD was performed using double-sided adhesive, which was cut to expose the contact areas between the electrodes as showed in Fig. 4 (a). The final version of assembled Multi-µEPaD is presented in Fig. 4 (b). Therefore, it was composed of 16 channels circularly distributed around to the sample injection point, being the sample homogenously transported to the 16 WEs, where all 16 sensing measurements were simultaneously carried out.

Insert Fig. 4

2.3. Biosensor architecture preparation

The as constructed screen printed WEs were previously modified with chitosan (CTS), carbon black (CB) and glucose oxidase (GOx) prior assembly the Multi-µEPaD. The modification strategy was based on the deposition of films on WEs from an aqueous dispersion containing 1 mg of CB, 5×10^{-5} L of a 1.0×10^{-3} L FCA solution and 9.5×10^{-4} L of a 0.02 % CTS (w/v) solution. The choice of CTS was based on the ability of this biopolymer to form stable aqueous dispersions of carbon nanomaterials, as well as the generation of homogeneous and stable films on the electrode surface [38]. After

preparation of the dispersion in the ultrasonic bath for 60 minutes, the GOx (7500 U, 48.4 mg) enzyme was added to 1.0 mL of the above dispersion and the obtained mixture subjected to mechanical stirring for an additional period of 30 minutes. An aliquot of 2×10^{-6} L of the dispersion was then deposited on each WE and dried at room temperature, thereby obtaining the biosensor architecture for glucose detection.

3. Results and discussion

3.1. Electrochemical performance of Multi-µEPaD

The evaluation of Multi-µEPaD electrochemical performance was carried out by adding an aliquot of 65 µL of 1.0×10^{-3} mol L^{-1} FCA in 0.1 mol L^{-1} KCl, as supporting electrolyte in the sample spot. FCA worked as a redox probe as it has a well-established electrochemical behavior, consisting of a reversible redox process with defined anodic and cathodic peaks observed through cyclic voltammetry (CV) assays [39]. The FCA responsivity in the proposed Multi-µEPaD was sequentially monitored by using four different electrochemical techniques: CV (channels of 1 to 4); differential pulse voltammetry (DPV) (channels of 5 to 8); square-wave voltammetry (SWV) (channels of 9 to 12) and chronoamperometry (channels of 13 to 16). The obtained results are shown in Fig. 5 (a-d).

The typical FCA electrochemical response was verified in all cases. The relative standard deviation (RSD) was calculated for the obtained analytical signals (peak currents in the case of voltammetric measurements and steady-currents for chronoamperometry). Doing this, the following RSD values were obtained: 3.6% for CV (Fig. 5 (a)), 4.7% for SWV (Fig. 5 (b)), 3.9% for DPV (Fig. 5 (c)) and 4.5% for chronoamperometry (Fig. 5 (d)). Moreover, to investigate the repeatability between

different devices, four Multi-µEPaDs were applied to the same described assays routine. In this case, the recorded RSD percentages did not exceed 5.0%. This set of data made clear that the desired performance of the device has been achieved to use it for multi-techniques applications using a single sample aliquot to perform the 16 independent measurements.

Insert Fig. 5

3.2. Glucose biosensing

The glucose biosensing was achieved in this research by exploring a second-generation biosensor strategy, which FCA was the selected electron mediator. Thus, FCA was confined on the WE surface within a CTS film together to CB nanoparticles and GOx enzyme. CB nanoparticles were added to the CTS film in order to ensure the electrical contact and a fast electron transfer rate and GOx enzyme acted as the biological component sensitive to glucose. The biosensor response towards glucose was explored from CV assays carried out using a Multi-µEPaD constructed with the modified WEs when an aliquot of a 10^{-2} mol L^{-1} glucose solution prepared in 0.1 mol L^{-1} NaCl, as the supporting electrolyte was added on the sample spot. The CVs were recorded using WEs modified with and without the GOx enzyme, and the obtained CVs are shown in Fig. 6. Doing this, it was verified that in the absence of the GOx enzyme within the film, the typical CV profile corresponded to the Fe^{3+}/Fe^{2+} [40] redox pair of FCA probe was obtained. However, when GOx was incorporated into the WE modification, a clear biocatalytic effect was indirectly observed, with the anodic peak current of FCA increasing at same time as the cathodic peak current was suppressed.

Insert Fig. 6

The observed behavior is in accordance with the previously reported glucose biosensing mechanism for FCA as a GOx electrons mediator [41]. Scheme 1 shows the referred reaction mechanism. Thus, FCA probe acted as an electron mediator for the GOx enzyme active center ($FAD/FADH_2$) that reacted with the glucose in solution. Enzymatic activity provides the glucose oxidation to D-glucono-delta-1,5-lactone, which is readily hydrolyzed generating the gluconic acid. At the same time, FAD is reduced to $FADH_2$. The last is oxidized back to FAD by Fe (III) of FCA probe being, therefore, reduced to Fe [40]. The Fe [40] redox state of FCA is, then, electrochemically determined via anodic potential scanning and, the verified anodic peak current is directly proportional to the amount of glucose enzymatically oxidized.

From the preliminary studies by CV, several optimizations in the assays were carried out. Each optimization study was performed using a single device. The first step was the determination of the optimal concentration (number of units) of GOx per electrode. For this, four CB-CTS dispersions, each one containing a defined amount of GOx, were prepared so that each deposited film contained amounts of enzyme equal to 5, 10, 15 and 20 units per electrode, respectively. The higher current increment was obtained for the biosensor containing 15 units of GOx per electrode (Fig. S3 (a)). Then, aiming to determine glucose by chronoamperometry, a second optimization step was carried out to determine the optimum applied potential. Thus, current response dependence regarding the applied potential was evaluated in the range of +0.3 to +0.7 V. The current response presented a maximum intensity value at +0.6 V (Fig. S3 (b)) being, therefore, the selected applied potential to the next assays.

Under the optimized conditions, the analytical curve for glucose was constructed from glucose standard solutions of different concentrations using the Multi-μEPaD. For each glucose standard solution concentration, a different device was used, that is, for the

performance evaluation of Multi-µEPaD to glucose determination all 16 channels was used for the same technique (16 replicates). In Fig. 7 (a) are provided the chronoamperograms recorded toward different glucose concentrations. The analytical curve (Fig. 7 (b)) was linear in the glucose concentration range from 10^{-4} to 4×10^{-2} mol L^{-1} (*i.e.* 18.3 to 7212.0 mg dL^{-1}) with a limit of detection (LOD) of 3×10^{-5} mol L^{-1} (5.5 mg dL^{-1}). The LOD was determined by the relationship LOD = 3σ / m, where σ is the standard deviation of 10 measurements of the blank's signal and m is the analytical sensitivity (slope of analytical curve). These analytical parameters demonstrate to be promissory for the application of the proposed biosensor architecture in the analysis of clinical samples. The range of glucose concentration in human urine [42] are within the linear range obtained with the Multi-µEPaD , demonstrating the applicability of the device. In addition, the Multi-µEPaD was studied for real sample analysis, where urine samples were spiked with two different concentrations of GLU (2.5×10^{-3} mol L^{-1} and 10×10^{-3} mol L^{-1}) obtaining errors below 5% (Fig. S4). Moreover, the repeatability of the device was studied using a 5×10^{-3} mol L^{-1} GLU solution in 5 different Multi-µEPaDs, where the RSD obtained was 7.4%.

Insert Fig. 7

4. Conclusions

The disposable electrochemical paper-based microfluidic device proposed can be easily constructed using a cheap craft cutter printer and simple materials allowing a high throughput analysis with the sixteen independent microfluidic channels. The Multi-µEPaD demonstrated robustness through the electrochemical performance experiments (CV, SWV, DPV and chroamperometry) presenting RSD values lower than 5.0%. The determination of glucose in body fluids as a prove of concept using Multi-µEPaD was

successful performed in urine samples. In this, the device proved to be appropriate for glucose determination using chronoamperometry with satisfactory results.

Acknowledgments

The authors thank the grants #2016/10012-4, #2017/24053-7 and #2017/10118-0, São Paulo Research Foundation (FAPESP), Coordenação de Aperfeiçoamento de Pessoal de Nível Superior (CAPES) – Brazil – Finance Code 001 and grant #405546/2018-1 from CNPq.

References

[1] P. Wang, L.J. Kricka, Current and emerging trends in point-of-care technology and strategies for clinical validation and implementation, Clin. Chem. 64 (2018) 1439-1452.

[2] C.D.M. Campos, S.S.T. Gamage, J.M. Jackson, M.A. Witek, D.S. Park, M.C. Murphy, A.K. Godwin, S.A. Soper, Microfluidic-based solid phase extraction of cell free DNA, Lab Chip 18 (2018) 3459-3470.

[3] D. Evans, K.I. Papadimitriou, N. Vasilakis, P. Pantelidis, P. Kelleher, H. Morgan, T. Prodromakis, A novel microfluidic point-of-care biosensor system on printed circuit board for cytokine detection, Sensors 18 (2018) 1-14.

[4] Z.Y. He, N. Ranganathan, P. Li, Evaluating nanomedicine with microfluidics, Nanotechnology 29 (2018) 1-23.

[5] S.R. Pajoumshariati, M. Azizi, S.Y. Zhang, B. Dogan, K.W. Simpson, A. Abbaspourrad, A microfluidic-based model for spatially constrained culture of intestinal microbiota, Adv. Funct. Mater. 28 (2018) 1-12.

[6] Y.H. Piao, X.B. Wang, H.M. Xia, W.Q. Wang, Digital microfluidic platform for automated detection of human chorionic gonadotropin, Microfluid. Nanofluid. 23 (2019) 1-8.

[7] D. Yu, L. Tang, Z.Y. Dong, K.A. Loftis, Z.Y. Ding, J.J. Cheng, B.Y. Qin, J.T. Yan, W. Li, Effective reduction of non-specific binding of blood cells in a microfluidic chip for isolation of rare cancer cells, Biomater. Sci. 6 (2018) 2871-2880.

[8] K.A. Hyun, H. Gwak, J. Lee, B. Kwak, H.I. Jung, Salivary exosome and cell-free dna for cancer detection, Micromachines 9 (2018) 1-13.
[9] A. Kulasinghe, H.J. Wu, C. Punyadeera, M.E. Warkiani, The use of microfluidic technology for cancer applications and liquid biopsy, Micromachines 9 (2018) 1-22.

[10] Y.X. Sun, T.A. Haglund, A.J. Rogers, A.F. Ghanim, P. Sethu, Microfluidics technologies for blood-based cancer liquid biopsies, Anal. Chim. Acta 1012 (2018) 10-29.

[11] J.S. Lee, C.B. Park, Microfluidic dissociation and clearance of Alzheimer's beta-amyloid aggregates, Biomaterials 31 (2010) 6789-6795.

[12] T.D. Mai, D. Ferraro, N. Aboud, R. Renault, M. Serra, N.T. Tran, J.L. Viovy, C. Smadja, S. Descroix, M. Taverna, Single-step immunoassays and microfluidic droplet operation: Towards a versatile approach for detection of amyloid-beta peptide-based biomarkers of Alzheimer's disease, Sens. Actuators, B 255 (2018) 2126-2135.

[13] N. Maughan, L.M. Nguyen, S. Gamagedara, Microfluidic separation and electrochemical detection of serotonin using a portable lab-on-a-chip device, Anal. Bioanal. Electrochem. 7 (2015) 1-11.

[14] B. Nasseri, N. Soleimani, N. Rabiee, A. Kalbasi, M. Karimi, M.R. Hamblin, Point-of-care microfluidic devices for pathogen detection, Biosens. Bioelectron. 117 (2018) 112-128.

[15] E. Carrilho, A.W. Martinez, G.M. Whitesides, Understanding wax printing: a simple micropatterning process for paper-based microfluidics, Anal. Chem. 81 (2009) 7091-7095.

[16] Z. Nie, C.A. Nijhuis, J. Gong, X. Chen, A. Kumachev, A.W. Martinez, M. Narovlyansky, G.M. Whitesides, Electrochemical sensing in paper-based microfluidic devices, Lab Chip 10 (2010) 477-483.

[17] M. Sher, R. Zhuang, U. Demirci, W. Asghar, Paper-based analytical devices for clinical diagnosis: recent advances in the fabrication techniques and sensing mechanisms, Expert Rev. Mol. Diagn. 17 (2017) 351-366.

[18] R.A.G. de Oliveira, F. Camargo, N.C. Pesquero, R.C. Faria, A simple method to produce 2D and 3D microfluidic paper-based analytical devices for clinical analysis, Anal. Chim. Acta 957 (2017) 40-46.

[19] K. Kadimisetty, I.M. Mosa, S. Malla, J.E. Satterwhite-Warden, T.M. Kuhns, R.C. Faria, N.H. Lee, J.F. Rusling, 3D-printed supercapacitor-powered electrochemiluminescent protein immunoarray, Biosens. Bioelectron. 77 (2016) 188-193.

[20] X.K. Li, M. Soler, C. Szydzik, K. Khoshmanesh, J. Schmidt, G. Coukos, A. Mitchell, H. Altug, Label-free optofluidic nanobiosensor enables real-time analysis of single-cell cytokine secretion, Small 14 (2018) 1-11.

[21] M.G. Mauk, J.Z. Song, C.C. Liu, H.H. Bau, Simple approaches to minimally-instrumented, microfluidic-based point-of-care nucleic acid amplification tests, Biosensors (Basel) 8 (2018) 1-30.

[22] A. Sayad, F. Ibrahim, S.M. Uddin, J. Cho, M. Madou, K.L. Thong, A microdevice for rapid, monoplex and colorimetric detection of foodborne pathogens using a centrifugal microfluidic platform, Biosens. Bioelectron. 100 (2018) 96-104.

[23] R. Kwapiszewski, M. Skolimowski, K. Ziolkowska, E. Jedrych, M. Chudy, A. Dybko, Z. Brzozka, A microfluidic device with fluorimetric detection for intracellular components analysis, Biomed. Microdevices 13 (2011) 431-440.

[24] R. Singh, S. Chopra, C. Graham, L. Nelson, R. Ng, M. Nuffer, P. Vadlamani, S. Norton, V. Pamula, Demonstration of a digital microfluidic platform for the high throughput analysis of 12 discrete fluorimetric enzyme assays using a single newborn dried blood spot punch, Mol. Genet. Metab. 12 (2018) S132-S132.

[25] Q. Zhang, X.W. Tang, F.H. Hou, J.P. Yang, Z.Y. Xie, Z.Y. Cheng, Fluorimetric urease inhibition assay on a multilayer microfluidic chip with immunoaffinity immobilized enzyme reactors, Anal. Biochem. 441(2013) 51-57.

[26] M. Amiri, A. Bezaatpour, H. Jafari, R. Boukherroub, S. Szunerits, Electrochemical methodologies for the detection of pathogens, ACS Sens. 3 (2018) 1069-1086.

[27] L. Farzin, M. Shamsipur, L. Samandari, S. Sheibani, Recent advances in designing nanomaterial based biointerfaces for electrochemical biosensing cardiovascular biomarkers, J. Pharm. Biomed. Anal. 161 (2018) 344-376.

[28] F.H. Cincotto, E.L. Fava, F.C. Moraes, O. Fatibello-Filho, R.C. Faria, A new disposable microfluidic electrochemical paper-based device for the simultaneous determination of clinical biomarkers, Talanta 195 (2019) 62-68.

[29] T.R. de Oliveira, W.T. Fonseca, G. de Oliveira Setti, R.C. Faria, Fast and flexible strategy to produce electrochemical paper-based analytical devices using a craft cutter printer to create wax barrier and screen-printed electrodes, Talanta 195 (2019) 480-489.

[30] F. Arduini, S. Cinti, V. Caratelli, L. Amendola, G. Palleschi, D. Moscone, Origami multiple paper-based electrochemical biosensors for pesticide detection, Biosens. Bioelectron. 126 (2019) 346-354.

[31] S. Boonkaew, S. Chaiyo, S. Jampasa, S. Rengpipat, W. Siangproh, O. Chailapakul, An origami paper-based electrochemical immunoassay for the C-reactive protein using a screen-printed carbon electrode modified with graphene and gold nanoparticles, Microchim. Acta 186 (2019) 1-10.

[32] S. Dalirirad, A.J. Steckl, Aptamer-based lateral flow assay for point of care cortisol detection in sweat, Sens. Actuators, B 283 (2019) 79-86.

[33] P. Kassal, M. Sigurnjak, I.M. Steinberg, Paper-based ion-selective optodes for continuous sensing: Reversible potassium ion monitoring, Talanta 193 (2019) 51-55.

[34] N. Ruecha, K. Shin, O. Chailapakul, N. Rodthongkum, Label-free paper-based electrochemical impedance immunosensor for human interferon gamma detection, Sens. Actuators, B 279 (2019) 298-304.

[35] S. Ge, L. Ge, M. Yan, X. Song, J. Yu, J. Huang, A disposable paper-based electrochemical sensor with an addressable electrode array for cancer screening, Chem. Commun. 48 (2012) 9397-9399.

[36] A.S. Afonso, C.V. Uliana, D.H. Martucci, R.C. Faria, Simple and rapid fabrication of disposable carbon-based electrochemical cells using an electronic craft cutter for sensor and biosensor applications, Talanta 146 (2016) 381-387.

[37] C.V. Uliana, C.R. Peverari, A.S. Afonso, M.R. Cominetti, R.C. Faria, Fully disposable microfluidic electrochemical device for detection of estrogen receptor alpha breast cancer biomarker, Biosens. Bioelectron. 99 (2018) 156-162.

[38] A. Blagg, O.P. Perez, R. Valentin, Effect of carbon black and silver nanoparticle loading on the structural and thermo-mechanical properties of chitosan-based films, Nanotechnology 1 (2012) 628-631.

[39] S. McCormack, N.R. Russell, J.F. Cassidy, Cyclic voltammetry of ferrocene carboxylic-acid cyclodextrin inclusion complexes, Electrochim. Acta 37 (1992) 1939-1944.

[40] K. Yoshimura, K. Tsukamoto, M. Okazaki, V.M. Virador, T.-C. Lei, Y. Suzuki, G. Uchida, Y. Kitano, K. Harii, Effects of all-trans retinoic acid on melanogenesis in pigmented skin equivalents and monolayer culture of melanocytes, J. Dermatol. Sci. Suppl 1 (2001) S68-75.

[41] E.A. Gutierrez, A.M. Wallraf, A. Balaceanu, M. Bocola, M.D. Davari, T. Meier, H. Duefel, U. Schwaneberg, How to engineer glucose oxidase for mediated electron transfer, Biotechnol. Bioeng. 115 (2018) 2405-2415.

[42] P. Sharma, P. Sharan, Design of photonic crystal-based biosensor for detection of glucose concentration in urine, IEEE Sens. J. 15 (2015) 1035-1042.

Figure captions

Fig. 1. (a) The hexadecagon model designed for the microfluidic pathway and **(b)** homogeneous elution of 1.0 $\times 10^{-3}$ mol L^{-1} Allura red dye solution in the microfluidic pathway.

Fig. 2. Schematic representation of construction process of electrodes (in this example the WEs and RE) is based on screen printing procedure, consisting of the following steps: **(1)** fixing the vinyl adhesive onto polyester sheet; **(2)** cutting the adhesive for the desired design followed by carbon conductive ink deposition; **(3)** removal of the adhesive after the inks have been dried and; **(4)** batch of ready electrodes to assemble the microfluidic device.

Fig. 3. (a) Design of the WEs/Res and **(b)** CE layers.

Fig. 4. (a) Steps for device layer assembly. **(b)** Photography of assembled µMULTI-µEPAD.

Fig. 5. Results obtained with the multiplexed analysis for the µMulti-µEPAD and the electrochemical probe 1.0 $\times 10^{-3}$ mol L^{-1} FCA in 0.1 mol L^{-1} KCl using **(a)** CV (*scan rate* = 50 mV s^{-1}).; **(b)** SWV (*frequency* = 80 Hz; *amplitude* = 90 mV and *potential increment* = 1 mV); **(c)** DPV (*scan rate* = 5 mV s^{-1}, *amplitude* = 90 mV and *modulation time* = 5 ms) and **(d)** Chronoamperometry (*applied potential* = 200 mV).

Fig. 6. CVs obtained for 10^{-2} mol L^{-1} glucose solution in 0.1 mol L^{-1} NaCl using the μMULTI-μEPAD containing modified WEs with (presence) and without (absence) of immobilized GOx enzyme. *Scan rate* = 50 mV s^{-1}.

Fig. 7. (a) Chronoamperograms obtained for different glucose concentrations (1: 0.0; 2: 0.1; 3: 0.5; 4: 1.0; 5: 5.0; 6: 10.0; 7: 20.0; 8: 30.0 and 9: 40.0(×10^{-3} mol L^{-1}) in 0.1 mol L^{-1} NaCl (Inset: amplification of the chronoamperograms recorded in the concentration range of 0.0 to 5.0×10^{-3} mol L^{-1}). Applied potential = +0.6 V. **(b)** Respective analytical curve (Background-corrected current *versus* [Glucose]).

Scheme captions

Scheme 1. Proposed mechanism for the biocatalytic oxidation of glucose solution mediated by FCA redox probe.

Figures

Fig. 1

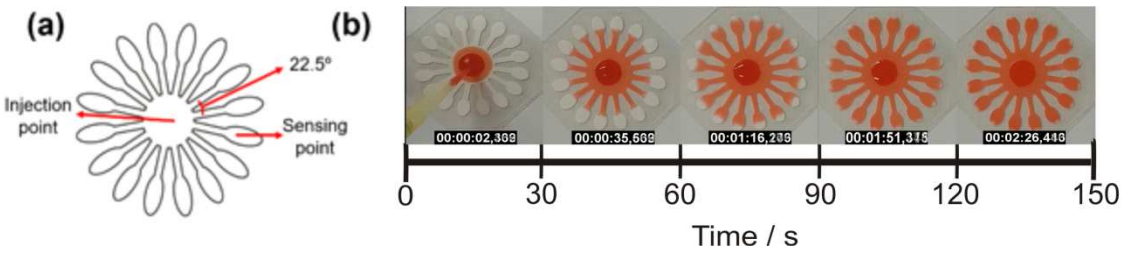

Fig. 2

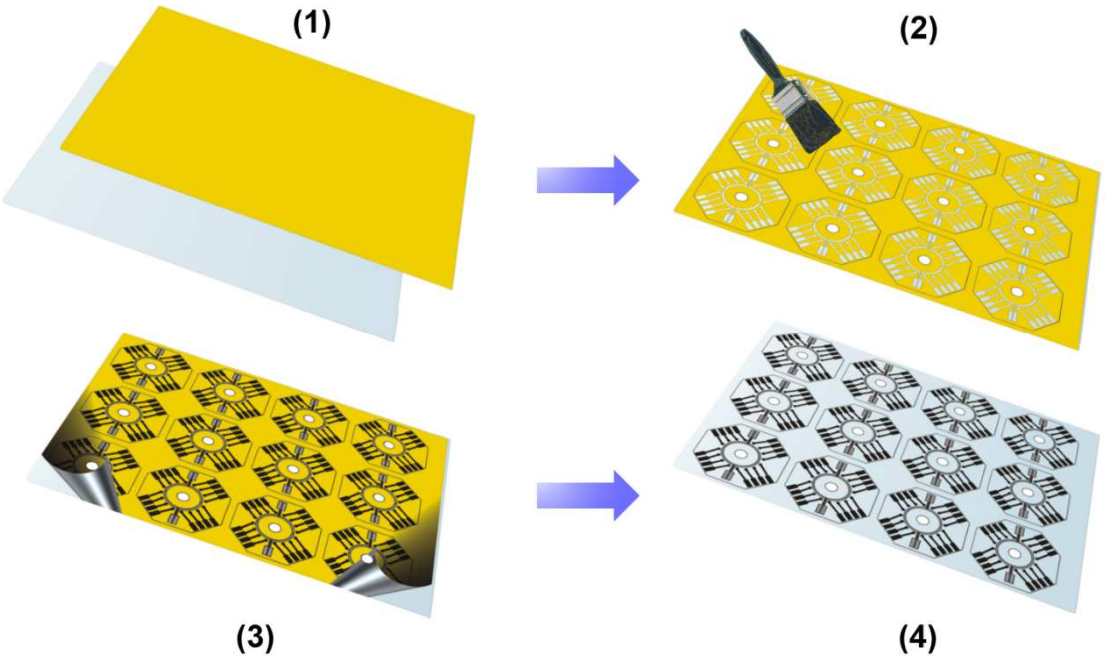

Fig. 3

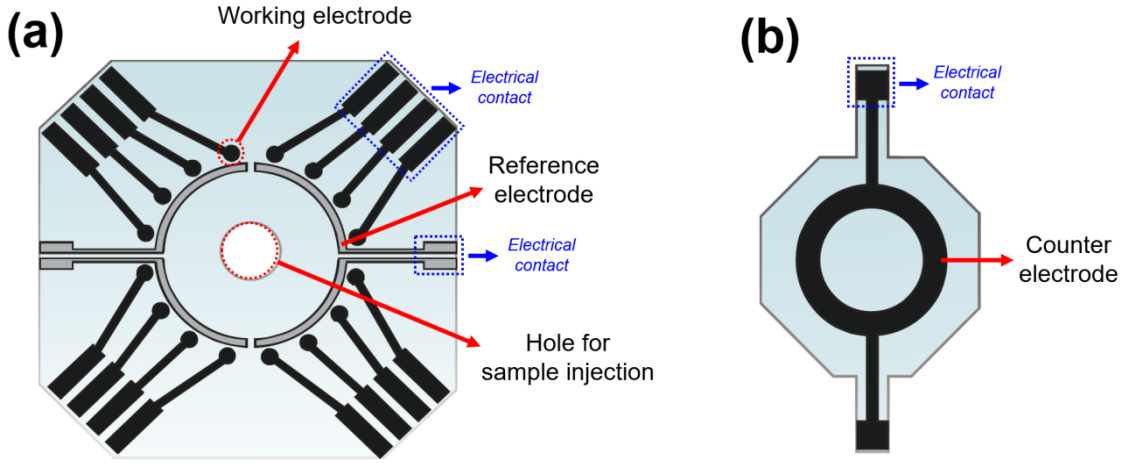
(a)
Working electrode
Electrical contact
Reference electrode
Electrical contact
Hole for sample injection
(b)
Electrical contact
Counter electrode

Fig. 4

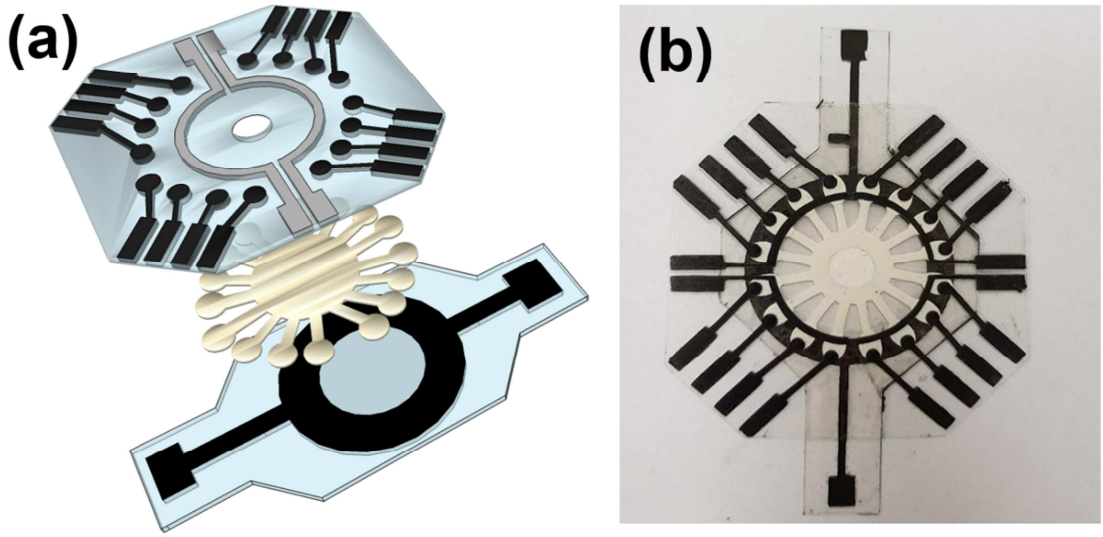
(a)
(b)

Fig. 5

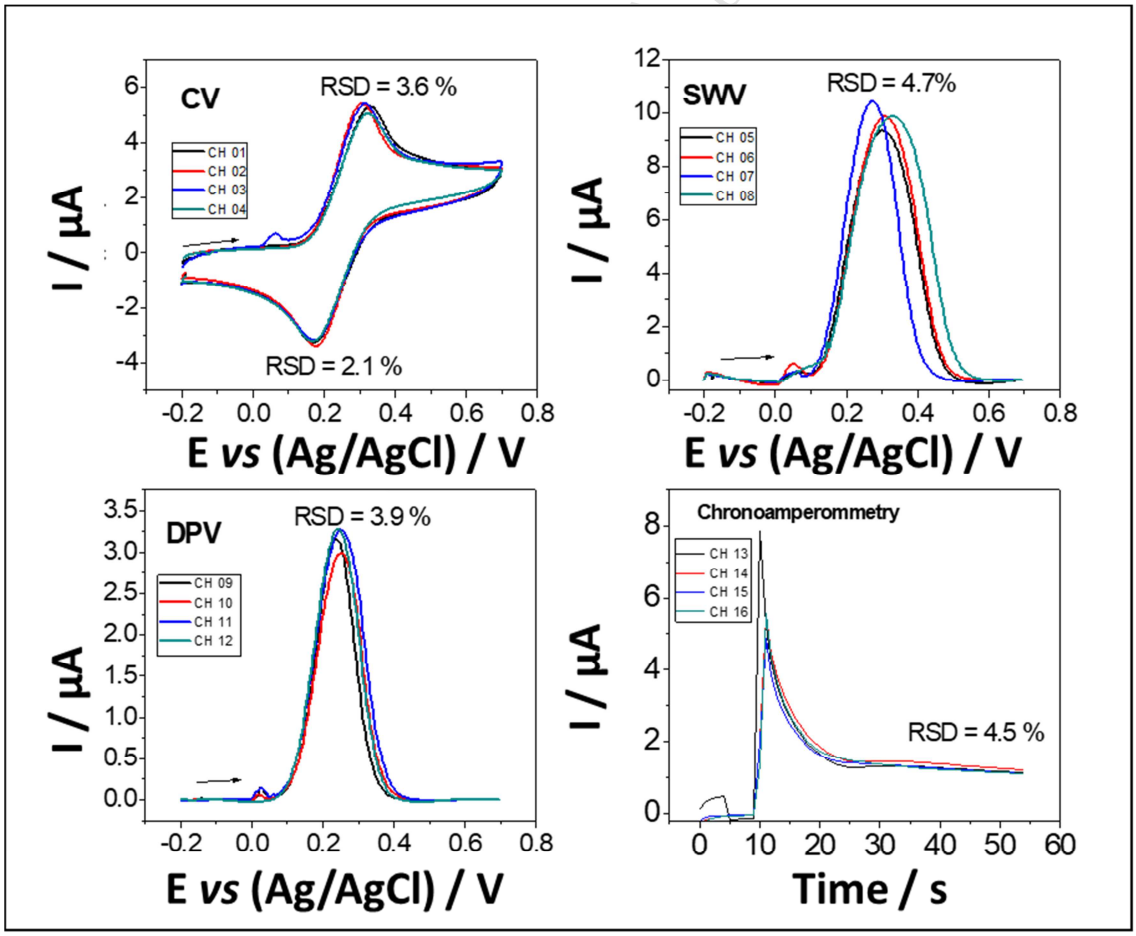
CV
RSD = 3.6 %
RSD = 2.1 %
CH 01
CH 02
CH 03
CH 04
I / µA
E vs (Ag/AgCl) / V
SWV
RSD = 4.7%
CH 05
CH 06
CH 07
CH 08
I / µA
E vs (Ag/AgCl) / V
DPV
RSD = 3.9 %
CH 09
CH 10
CH 11
CH 12
I / µA
E vs (Ag/AgCl) / V
Chronoamperommetry
CH 13
CH 14
CH 15
CH 16
RSD = 4.5 %
I / µA
Time / s

Fig. 6

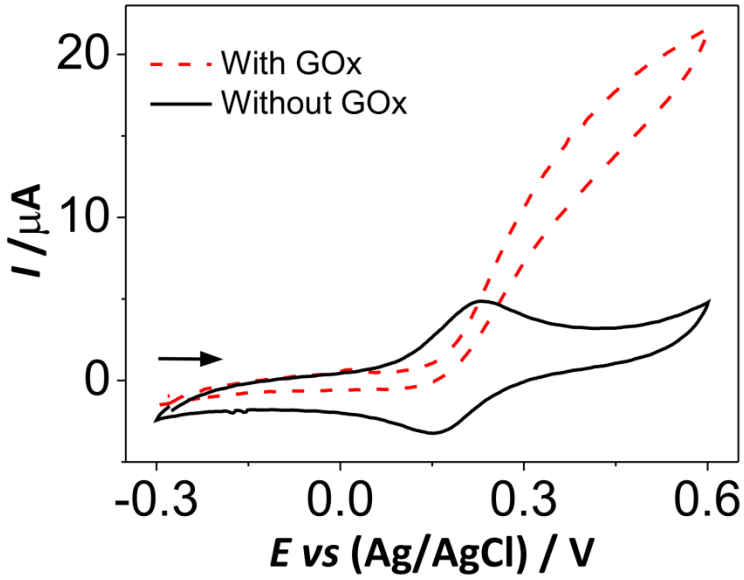

Figure 7

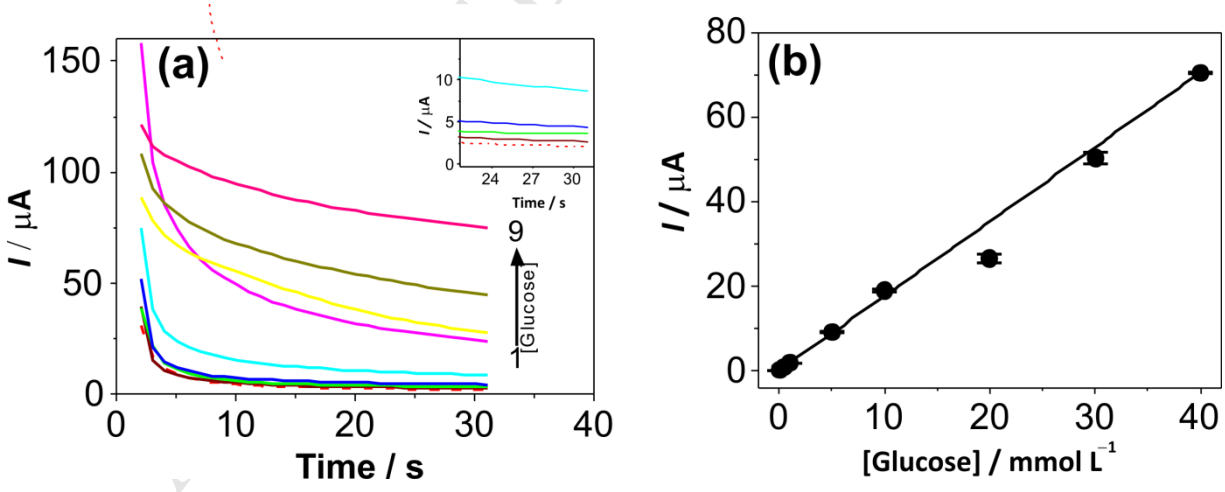

Scheme 1

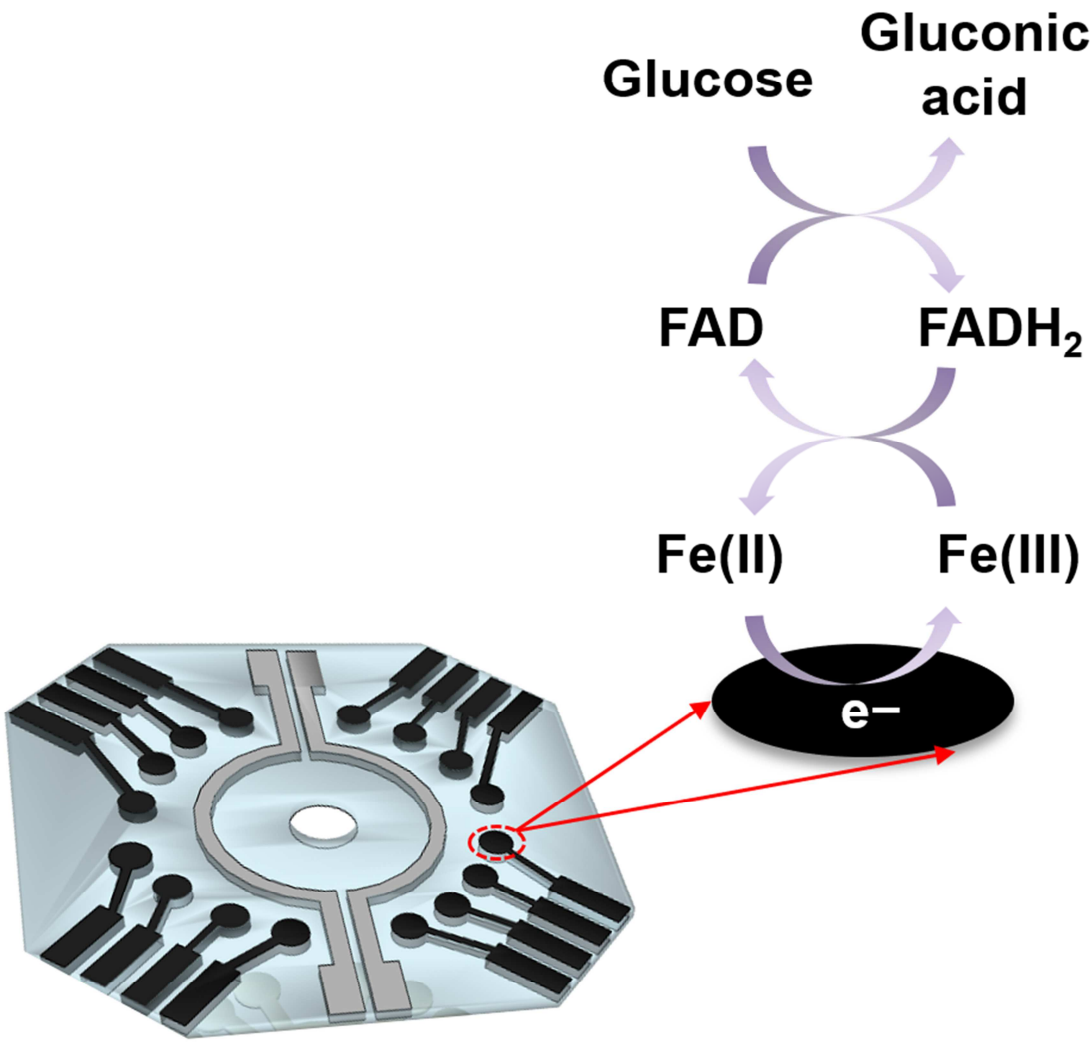

Highlights

- The novel sensoring platform proposed presents low cost of fabrication, allows the multiplexed analysis with high throughput for small sample volume (75 µL). and is disposable;
- Compounds of interest for clinical analysis can be detected with 16 independent microfluidic channels in multiplexed analysis;
- The non-invasive glucose determination in urine was adopted as proof of concept, demonstrating high performance and easily operation for a small sample volume.